Materials and Design 35 (2012) 685–690

Contents lists available at SciVerse ScienceDirect

Materials and Design

journal homepage: www.elsevier.com/locate/matdes

Short Communication

Improvement of mechanical properties in severely plastically deformed Ni–Cr alloy

K.H. Song *, H.S. Kim, W.Y. Kim

Korea Institute of Industrial Technology, 7-47, Songdo-Dong, Yeonsu-gu, Incheon 406-840, Republic of Korea

ARTICLE INFO

Article history:
Received 6 July 2011
Accepted 18 October 2011
Available online 28 October 2011

ABSTRACT

This study was carried out to evaluate the grain refining and mechanical properties in alloys that undergo severe plastic deformation (SPD). Conventional rolling (CR) and cross-roll rolling (CRR) were introduced as methods for SPD, and a Ni–20Cr alloy was selected as the experimental material. The materials were cold rolled to 90% thickness reduction and subsequently annealed at 700 °C for 30 min to obtain the fully recrystallized microstructure. The annealed materials after cold rolling were assessed through electron backscattered diffraction (EBSD) analysis to investigate the grain boundary characteristic distributions (GBCDs). The CRR process was more effective than the CR process in developing grain refinement; the grain size decreased from 70 μm in the initial material to 4.2 μm (CR) and 2.4 μm (CRR), respectively. The grain refinement affected mechanical properties such as microhardness, yield, and tensile strength, which were significantly increased relative to the initial material.

1. Introduction

Chino et al. [1] proposed the cross-roll rolling (CRR) process, which is a new rolling process in which the roll axes are tilted against the transverse direction (TD) in the rolling direction (RD)–TD plane. This new rolling process can impose a higher effective strain than that of the conventional rolling (CR), which results mainly from shear deformation in ε_{23} [2]. Generally, the effective strain imposed on the material during deformation directly affects the resulting grain size through heat treatment. In other words, a higher effective strain can produce a finer grain size [2]. The Ni base alloy used in this study has an intermediate stacking fault energy (SFE), between that of Cu and Al alloys; however, an increase in the Cr content of the Ni matrix leads to a gradual decrease in SFE [3,4]. Materials with low SFE are known to achieve a finer grain size than materials with high SFE through SPD and subsequent annealing because of the large number of nuclei sites in the former [3,4]. Therefore, the CRR process with higher effective strain than that of the CR process can result in smaller grain size and increased mechanical properties. Lately, SPD processes such as equal channel angular pressing (ECAP), high-pressure torsion (HPT), and high-speed-ratio differential speed rolling (HRDSR) have been studied to achieve high strength via the decrease in grain size [5–10]. However, research on the CRR process on Ni–Cr alloys has not been carried out thus far.

The present study evaluated the enhancement in microstructure and mechanical properties in severely plastically deformed Ni–20Cr by CRR relative to the CR-processed material, and discussed the effect of the effective strain on grain refinement and mechanical properties.

2. Experimental procedures

The material used in this study was a Ni–20Cr alloy with dimensions of 30 mm × 50 mm × 8 mm, and its chemical composition is shown in Table 1. The homogenized microstructure was obtained by solution treatment at 1000 °C for 1 h. The specimen was mechanically ground to remove the surface oxidation and cold rolled to 90% thickness reduction without lubrication to maximize the shear strain. In particular, the CRR was carried out while maintaining the roll mill condition in which the roll axes were tilted 5° from the transverse direction (TD) in the RD–TD plane. To observe the microstructures of the cold-rolled materials prepared by CR and CRR, transmission electron microscopy (TEM) was introduced. Cold-rolled sheets were subsequently cut to 3 mm discs, mechanically ground to 80 μm, and jet-polished to 10 μm using a solution of 10 ml perchloric acid and 90 ml methanol at −30 °C. TEM on thinned specimens was carried out at 200 kV.

For annealing the cold-rolled material, the specimens were reduced to 5 mm × 5 mm, and subsequently annealed at 700 °C for 30 min to obtain the fully recrystallized microstructure. Electron backscattered diffraction (EBSD) was used to analyze the grain size, grain boundary characteristic distributions (GBCDs), and textures on annealed materials. For this, the specimens were additionally polished by a vibratory polisher, and the surfaces were then analyzed using orientation image mapping incorporated in scanning electron microscopy (SEM). For analyzing the fractured surfaces, SEM analysis was introduced, and the fracture shape and dimple size in 10 points at each fractured sample were evaluated. To evaluate the mechanical properties, Vickers microhardness and tensile strength tests were also employed. The former tests were carried out on cross sections of the specimens with a load of 9.8 N and a dwell time of 15 s. Tensile test specimens were used to evaluate

* Corresponding author. Tel.: +82 32 850 0395; fax: +82 32 850 0410.
E-mail address: skhyun7@nate.com (K.H. Song).

0261-3069/$ - see front matter © 2011 Elsevier Ltd. All rights reserved.
doi:10.1016/j.matdes.2011.10.029

Table 1
Details of chemical composition on Ni–20Cr alloy.

Element	Ni	Cr	Si	Mn	S	C
Mass%	Bal.	19.98	0.015	0.02	0.008	0.08

the transverse tensile strength of the cold-rolled and recrystallized materials (Fig. 1). Tensile testing was conducted at room temperature and at $1 \times 10^{-2}\ S^{-1}$.

3. Results and discussion

Fig. 2 shows the grain boundary map, grain size distribution, and grain boundary misorientation angle distribution, acquired by the EBSD analysis in the initial material. The initial material consisted of equiaxed grains, including a large amount of annealing twins, as shown in Fig. 2a. At this state, the average grain size was 70 μm and the range was between 2.4 and 130 μm. Fig. 2b shows the heterogeneously distributed grains. In all misorientation angle fractions, the high-angle grain boundary was more than 90%, and the 60° distribution showed the highest fraction of the misorientation angle distribution, as shown in Fig. 2c. This was identified as annealing twin boundaries, which are well known in materials with lower stacking fault energy, as in fcc metals.

Severely deformed microstructures by CR and CRR are shown in Fig. 3. In the 90CR-processed material, the elongated 50- to 200-nm wide grains, along the rolling direction, were distributed, as shown in Fig. 3a. In contrast, the 90CRR-processed material consisted of more equiaxed grains relative to the 90CR-processed material, as shown in Fig. 3b. Moreover, the selected area diffraction pattern of 90CRR showed more rings than that of 90CR, which corresponds to a higher fraction in the high-angle boundary distribution. However, a large amount of dislocations in the microstructure due to large strain was observed at all conditions.

Grain boundary maps and the grain boundary misorientation angle distribution of cold-rolled and annealed materials are shown in Fig. 4. Application of cold rolling effectively improved the grain refinement through heat treatment. As a result, the CR-processed and annealed material consisted of grains between 0.2 and 12.2 μm with an average size of 4.2 μm, which is significantly smaller than that of initial material, as shown in Fig. 4a. The CRR material was more affected by grain refining, and the grains ranged from 0.2 to 9 μm with an average size of 2.4 μm, as shown in Fig. 4b. In the misorientation angle distribution, the high-angle grain boundaries occupied more than 95% at all conditions (Fig. 4c and d). In addition, the 60° distribution showed the highest fraction at all conditions, which was identified as annealing twin boundaries similar to that of the initial material. The change in grain size is shown in Fig. 5.

The change in the Vickers microhardness due to cold rolling and annealing is shown in Fig. 6. The application of cold rolling led to an increase in microhardness, for example, the microhardness increased from 116 Hv in the initial material to 348 and 427 Hv in CR and CRR, respectively. The microhardness was notably higher in CRR. In the case of the annealed materials, the microhardness was 200 Hv in CR and 266 Hv in CRR, respectively. Similarly to the cold rolled materials the higher values was seen in the CRR material.

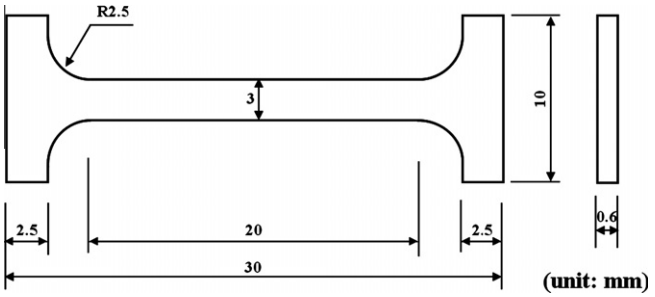

Fig. 1. Configuration of the transverse tensile specimen used in this study.

The tensile properties of the initial cold rolled and annealed materials are shown in Fig. 7. At initial material, yield and tensile strengths were 42 and 418 MPa, respectively, with an elongation of 50%. The application of cold rolling notably increased the yield and tensile strength. For instance, the CR- and CRR-processed materials showed yield strength of 823 and 1056 MPa and tensile strength of 1010 and 1160 MPa, respectively. However, their elongation decreased to 6.5% (CR) and 5.7% (CRR), respectively. In the annealed materials, the yield and tensile strength of the CR material was 201 and 509 MPa, respectively, with an elongation of 34%. The yield and tensile strength of the CRR material was 351 and 584 MPa, respectively, with an elongation of 32%. These results show a significant increase in yield strength without a remarkable decrease in elongation when compared to the CR material. Mechanical properties observed in this study are simply shown in Table 2.

The scanning electron micrographs of the fracture surface are shown in Fig. 8. At all conditions, the fracture process was ductile with failure mechanisms arising from nucleation, growth, and link-up of voids, as shown in the figures. However, the CRR-processed and annealed material showed a slightly larger dimple size than that of the CR-processed and annealed material regardless of grain size. In the annealed materials (Fig. 4), the average grain size was 4.2 μm in CR and 2.4 μm in CRR, however, the dimple size was from 0.5 to 4 μm in the CR and from 1 to 6 μm in the CRR, respectively, as shown in Fig. 8.

The change in the texture distribution of the initial material, and the cold rolled and subsequently annealed materials is shown in Fig. 9. In the initial material, the grains were densely distributed at ⟨001⟩//ND, as shown in Fig. 9a. The CR-processed and annealed material showed densely distributed grains at ⟨001⟩//ND, similar to that of the initial material, as shown in Fig. 9b. However, the grains in the CRR-processed and annealed material were densely distributed at ⟨111⟩//ND, as shown in Fig. 9c.

The material used in this study was a Ni–20Cr alloy with low SFE. Generally, Ni has an intermediate SFE; however, the increase in the Cr content of the Ni matrix decreased the SFE of the material [11]. This lower SFE material effectively enhanced the grain refinement relative to that of the higher SFE material. Generally, low SFE materials undergo discontinuous recrystallization rather than continuous recrystallization by means of dynamic recovery, due to difficulties in the rearrangement of dislocations [12,13]. Therefore, the high density of stored energy can be imposed to materials by SPD, when compared to high SFE materials, which results in more recrystallization nuclei sites. Consequently, this can result in significantly smaller grain size in both processes.

The application of the SPD process such as CR and CRR leads to notable grain refinement. As a result, the average grain size significantly decreased from 70 μm in the initial material to 4.2 and 2.4 μm in CR and CRR, respectively, as shown in Figs. 2 and 4. In particular, the CRR-processed material had a smaller size than the CR-processed material. This can be explained in terms of the effective strain, which was imposed during deformation. Generally, a large effective strain imposed on a material can lead to smaller grains through heat treatment. The CRR process applied in this study has a larger effective strain than the CR process due to shear deformation in ε_{23} [14,15]. As is known theoretically, CR mainly imposes the deformation with $\varepsilon_{11} = -\varepsilon_{33}$ and $\varepsilon_{22} = \varepsilon_{12} = \varepsilon_{13} = \varepsilon_{23} = 0$ whereas in the practical rolling process ε_{13} is not zero. However, the CRR process anticipates the shear deformation in ε_{12}, ε_{13}, and ε_{23}, which